Following Potential Vorticity and Pollution across the Pacific – Spring 2001: Atmospheric Layers Observed during TRACE-P

Yuanlong Hu, Reginald E. Newell*, R. Alan Plumb, and William Heres
Department of Earth, Atmospheric and Planetary Sciences,
Massachusetts Institute of Technology, Cambridge, MA

Valérie Thouret
Laboratoire d'Aérologie, Université-Paul Sabatier, Toulouse, France

Edward V. Browell, Marta A. Fenn, and David J. Westberg
NASA, Langley Research Center, Hampton, VA

Corresponding Author: Yuanlong Hu
e-mail: hyl@mit.edu, ph: (617) 253-6386, fax: (617) 258-9819

Submitted for TRACE-P 2nd Special Issue

Journal of Geophysical Research-Atmospheres

October 31, 2003

(*) Deceased.

Abstract.

We have noted previously that atmospheric layer structure often occurred when stratospheric air moved into the troposphere. About 50% of the tropospheric layers originate from stratospheric sources, sometimes with these layers topping the layer formed by pollution from the surface [*Newell et al*., 1994; *Stoller et al*., 1999]. A good case of the latter was reported by *Cho et al*. [2001]. Occasionally the layers formed by pollution sources seem to dominate over those instigated by stratospheric folding, though this may be in doubt, and this possibly occurs over the Pacific in the spring of 2001 as noted in the NASA's Global Tropospheric Experiment (GTE) Transport and Chemical Evolution Over the Pacific Experiment (TRACE-P) period. We have summarized the properties of layers measured during the mission carried out between February and April 2001, using in situ measurements of water vapor, ozone, carbon monoxide, and methane. A modified mode-based method is adopted to define a layer. A combined total of 311 vertical profiles taken from the DC-8 and P-3B aircraft were sampled and 466 layers were identified using O_3 and H_2O, while 315 layers were found using the combinations of four constituent deviations (i.e., O_3, H_2O, CO, and CH_4) to incorporate more information of layer sources. The average thickness of a layer is 0.56 kilometers and the average altitude is 5.3 kilometers. Those layers occupied about 21% of the total atmosphere during the period. When water vapor mixing ratio was low and ozone was high, there were about 70 cases when carbon monoxide and methane were low, suggesting that these were stratospheric layers. The statistical results were also compared to those from previous GTE campaigns (i.e., the four Pacific Exploratory Missions: PEM-West A and B; PEM-Tropics A and B), as well as other extensive aircraft observations from the

Measurement of Ozone and Water Vapor by Airbus In-Service Aircraft (MOZAIC) program. A case study is given that highlights a "super layer" found during DC-8 transit Flight 5 for 27 February from Hawaii to Guam. Here Potential Vorticity (PV) diagnostics are applied to evaluate the control by the large-scale environment of stratospheric intrusions and more importantly, to assess their influence on the tropospheric layer structure. Using meteorological analysis and backward trajectories, we illustrate that stratospheric folding events in conjunction with the surface features can produce a region along the southern flank of oceanic subtropical highs that hosts the Asian polluted air being trapped at low troposphere for this season.

1. Introduction

The description of NASA's TRACE-P has been presented by *Jacob et al*. [2003]. *Fuelberg et al.* [2003] give an overview of the meteorological environment during the period. Meteorological events play a major role in atmospheric chemistry, and this is especially true for constituents such as tropospheric ozone which can add to the greenhouse effect on one hand and contribute to the regulation of the atmospheric oxidizing (cleansing) capacity on the other. The full range of meteorological scales, from the micrometeorological to the planetary, may be involved in the spatial and temporal distribution of substances with intermediate lifetime such as tropospheric ozone (meaning longer than a day and shorter than a few months).

Our main interest has been the potential vorticity and in the occurrence of pollution, particularly ozone, and their interactions, in the form of layers within the atmosphere. Rather than reciting these findings directly [e.g. *Newell et al.,* 1999], we have tried to

summarize them indirectly. The two aircraft used, the P3-B and the DC-8, have certain planned tasks set out roughly before the experiment and these were followed fairly closely. The fraction of the atmosphere explored was, in a sense, determined before the start of the mission. In this paper we seek to illustrate the dynamic relationship between the meteorological conditions which transport high ozone concentrations from both anthropogenic and natural sources. We would like to know where in this fraction were PV or O_3 found and how were they related. Section 2 describes the background information regarding the data set and layer identification methodology, and the trajectory model used in the study. Section 3 provides brief layer statistics that extends the coverage slightly from previous GTE missions and MOZAIC as well. A subdivision of layers according to the constituents used is also included. In section 4, we present a detailed case study for DC-8 Flight 5 during which a "super layer" was encountered during this transit flight on February 27 from Hawaii to Guam. In addition to a description of meteorological situation, we move towards an expansion of the parameters by including additional information such as potential vorticity. Conclutions and future research directions are discussed in section 5.

2. Background Information

2.1. Data and Layer Identification

TRACE-P data from 17 DC-8 flights (flight 4 to 20) and 21 P-3B flights (flight 4 to 24) were used to identify layers. Detailed data information and collecting methods can be found in *Jacob et al*. [2003]. There are about 8 quasi-vertical profiles per flight. For

TRACE-P, this leads to over about 1200 km of troposphere being vertically sampled. We use only profiles that sampled at least 2.5 vertical kilometers without interruption.

The layers were classified, as carried out previously by *Stoller et al*. [1999], *Newell et al*. [1999], and *Thouret et al*. [2000, 2001]. Layers in the vertical profiles made by the aircraft were identified from deviations exceeding specified thresholds from averaged background concentrations. These thresholds are set to ±10 ppbv for ozone; ±5% for relative humidity; and ±3 ppbv for both carbon monoxide and methane.

Global meteorological fields of the ECMWF analyses covering the TRACE-P period (from 00Z February 15 to 18Z March 1, 2001) were available to us with horizontal resolution of 1º × 1º, 60 model levels in the vertical (from surface up to 0.1hPa), and a temporal interval of 6 hours. They are used for PV diagnosis and other meteorological analysis.

2.2. Trajectory Model

The model used in the trajectory analysis is loosely based on the "Offline" trajectory package developed for the U.K. Universities Global Atmospheric Modeling Programme (UGAMP) [*Methven*, 1997; *Jackson et al*., 2001] which uses a standard 4^{th} order Runge-Kutta integration scheme with constant step size. While the "Offline" package performs its integration entirely on a sphere, our code does the same unless a particle is projected to lie between the northern-most of southern-most data point and a pole, in which case a special local Cartesian scheme is used [*Eluszkiewicz et al*., 1995].

3. Layers Observed during TRACE-P: Statistical Results

Water vapor and ozone were divided into four groups with anomalies processed from their averages (as seen in Table 1). They are exhibited geographically in Plate 1; clearly there is an abundance of layers in routes leading out of Hong Kong. The layers are colored according to their average altitude as noted. As before the main contribution comes from species that have high ozone and low water vapor (254 out of 466 layers, see Plate 2). The other three types are about equally distributed. If we expand the type 2 definition (high ozone and low water vapor) to include methane and carbon monoxide, then the high ozone, low water vapor, low carbon monoxide and low methane gives over 70 cases, while the high ozone, low water vapor, high carbon monoxide and high methane also give almost 70 cases. The former came directly from a stratospheric source and the latter could have been involved in a collision between layers with the stratospheric layer colliding from the top with the pollution layer [*Cho et al*., 2001]. This provides a separate way of using the layer distributions. Finally the layer thicknesses versus height do not show much variability.

Type 1 (Plate 3a) has ΔO_3 and ΔH_2O positive with the CO and CH_4 anomalies distributed among their four possibilities. The largest number, with 22 cases, was to see four types all with four positive anomalies. Five of these were found above 8 km, and could well have originated in the boundary layer.

Type 2A is a layer with (locally) O_3 high, H_2O low, and both CO and CH_4 high (Plate 3b). This could be a layer that has emerged from the stratosphere to the troposphere and then been superposed by downwards transit to continue with a polluted tropospheric layer. Type 2B could be a similar circumstance with a negative CH_4 anomaly; while

Type 2C could be a similar circumstance with a negative CO anomaly. Type 2D would be a clear cut stratospheric feature with both CO and CH_4 being diminished within the stratosphere. Out of this set then, three out of four types would be involved with layer collisions; only type 2D would be a clear-cut stratospheric layer.

Type 3 has an O_3 anomaly which is negative and an H_2O anomaly which is positive (Plate 3c), the largest value having both ΔCO and ΔCH_4 negative and the second largest having these two anomalies positive. One could speculate that the first combination denotes material that started in the boundary layer over the ocean, where O_3 anomaly is often negative. Three negatives, ΔO_3, ΔCO and ΔCH_4, could represent relatively clean air. Two positives, ΔCO and ΔCH_4, could represent polluted air.

Type 4 has both ΔO_3 and ΔH_2O values negative with the largest of the sub-categories having ΔCO and ΔCH_4 also negative (Plate 3d). This could be indicated to show a lack of pollution in an air mass that had spent some time in the upper troposphere away from sources. Positive methane or carbon monoxide deviation could indicate possible contamination with pollution. Overall, and as before, the main finding stands – that the coupled ΔO_3 positive and ΔH_2O negative give the largest contribution to the organization of the layers.

The data collected in Plate 3, following the combination of four tracers H_2O, O_3, CO, and CH_4, are summarized in Table 1. This resembles the table used by *Stoller et al.* [1999]. Layers 2A and 2D have the maximum number of observations about 70, out of the 315 total. A number of these layers have been involved in coupling, as we have previously mentioned. Probably only the rich O_3 and poor H_2O, CO and CH_4 layers came directly from the stratosphere.

The previous data, coupled with TRACE-P, are summarized in Table 2. MOZAIC data is still the main set of data but it is clear that the processes occurring elsewhere follow the trend of MOZAIC. Out of a total of 105,498 km profiles, 22,380 layers were sampled for a net coverage of 17%. This data is updated from a paper by *Newell et al.* [1999].

4. The "Super Layer" Case: DC-8 Flight 5 from Kona to Guam on 27 February 2001

4.1. Overview and Meteorological Setting

The case selected was DC-8 flight 5 for February 27, 2001 when it flew a near straight flight track from Kona, Hawaii to Guam, with extensive vertical profiling. A MOPITT (Measurements Of Pollution In The Troposphere) validation experiment was conducted [*Jacob et al*., 2003; *Heald et al*. (submitted manuscript, 2003)]. Plate 4 shows the along-track cross-section of Lidar ozone (in ppbv, color shaded) along with contoured potential temperature (Plate 4a) and potential vorticity (Plate 4b). There was an extensive layer about 3800 km long, from about 162˚W to 162˚E, which was observed and sampled repeatedly with ozone up to 80 ppbv and CO about 230 ppbv. Satellite water vapor imagery showed that the flight region was quite dry (Figure 1). The other pollutants in the layer, for example, HNO_3 (399 pptv maximum) and butane (39 pptv maximum) were not especially high so did not fall into a characteristic maximum tendency. Even the propane/ethane ratios were low (0.31 cp a maximum of 0.9) indicating fairly old data. It is little doubt that the high concentration of CO observed within this "super layer" was a result of favorable transport conditions that delivered pulses of anthropogenically polluted air to the lower troposphere.

Several other papers in the TRACE-P first special issue demonstrated that wave cyclones and associated cold fronts and warm conveyor belts (WCBs) are the principal mechanism for export of Asian pollution to the Pacific in spring [*Hannan et al*., 2003; *Carmichael et al.*, 2003; *Liu et al*., 2003].

Fuelberg et al. [2003] pointed out that meteorological conditions for TRACE-P were undergoing major changes since the February – April period marked the transition from winter to spring in the Northern Hemisphere, in addition to a quick decay of the La Nina (cold phase ENSO) condition. He went on to highlight this transition by examining the flow patterns during roughly the first half and the second half of the mission period. Similar to their approach, albeit a different time averaging frame, Figure 2a shows the mean sea level pressure for the period February 22 through March 1, 2001 that includes the DC-8 flight 5. The large-scale flow patterns over the Northern Hemisphere Pacific Basin are very similar to Figure 1a in *Fuelberg et al*. [2003] averaging for a longer period (between February 23 through March 17), i.e., a well-established Siberian high, an intense Aleutian cyclone, and a subtropical oceanic anticyclone between Hawaii and California, except that another oceanic anticyclone exists in the western Pacific subtropics that bridged the broad high pressure regions between the Asian continental high and the high system to the east of Hawaii, showing a predominant subsiding controlled by those high systems along the flight track which is consistent with the dry regions of the satellite image (see Figure 1). As we will show later, the location of this time-mean anticyclone plays an important role in forming the observed “super layer”. It is informative to examine the upper level waves and associated vorticity which originated over the East Asian continent for the same period since the upper level atmospheric

dynamics is necessary for the development of the frontal systems at the surface [*Holton,* 1992]. Figure 2b shows 257hPa ECMWF model level geopotential heights as contour lines and the vertical component of the relative vorticity, a measure of rotation, as a gray-scale field (dark region indicate large values of positive relative vorticity which represents cyclonic rotation), averaged between February 22 and March 1. A two-ridge, one-trough flow pattern is evident with one weak ridge in the subtropics to midlatitude near 140ºE, one strong ridge extending SW-NE from Hawaii towards the Bay of Alaska, and a strong trough over or ahead of the Aleutian low at the surface. The near collocation of lobes of positive and negative vorticity patches with those of ridges and troughs indicates the progressive nature of these systems. Indeed, during this period, this time-mean pattern was distorted by a cyclonic system moving offshore from China ENE towards the south of Japan starting around 00Z February 23 (figure not shown, but this is the same event mentioned by *Heald et al*. (submitted manuscript, 2003) that delivered the Asian polluted air). This system developed and deepened over the sea and merged eventually into the Aleutian cyclone by February 26. At 12Z February 24, a westward shift of location of the western subtropical high is obvious (see Figure 3a) due to this translating cyclone and the upper level trough had significantly amplified as shown in Figure 3b. Twenty four hours later (12Z February 25), a cutoff low was developed at the surface near 28ºN, 159ºW in association with this deepening upper level trough (figure not shown). The subtropical high was restored its strength and position by 12Z February 27. We hypothesize that the anthropogenic pollutants, along with the elevated O_3 concentration from both anthropogenic and natural origins (more specifically, from the

stratosphere. See next section) found in the "super layer" was largely due to this meteorological setting.

4.2. PV Perspective

The approximate conservation of potential vorticity is the single most powerful dynamical constrain on the atmospheric circulation (PV is exactly conserved following adiabatic and frictionless motion). PV methods have proven useful in understanding synoptic- and large-scale dynamics [*Holopainen et al*., 1982; *Wu and Emanuel*, 1995]. We calculated potential vorticity which can be evaluated as the product of two terms from the following equation:

$$Q = \left[f + \left(\frac{\partial u}{\partial y} \right)_\theta - \left(\frac{\partial v}{\partial x} \right)_\theta \right] \bullet \left[-g \frac{\partial \theta}{\partial p} \right]$$

Where Q represents potential vorticity, f is the Coriolis parameter, θ is the potential temperature, p is the pressure, g is the gravitational constant, u, v, x, and y follow their usual meanings. The first term on RHS is the vertical component of the absolute vorticity; the second term is a measure of the atmospheric static stability.

Layers of high PV, often accompanied by high O_3, are frequently found in the troposphere. Such layers sometimes possess low non-methan hydrocarbons also characteristic of the low stratosphere. Fission-products from nuclear weapon tests were previously used as a tracer for this type of air. *Danielsen* [1964, 1968] was a pioneer in this work for O_3, water vapor and radiocarbon and published extensively on the topic. In particular, *Danielsen et al.* [1987] proposed that atmospheric chemists should be able to use positive correlations of O_3 and PV and negative correlations of water vapor mixing ratio and PV to identify air of stratospheric origin. He further suggested that these

correlations might be used to derive quantitative estimates of stratospheric-tropospheric exchange. Air in the stratosphere has very high static stability (where temperature is constant or increases with height). According to the equation above, regions of high relative vorticity near the tropopause will be regions of high PV. Plotting the values of PV at relatively low tropospheric heights will include regions where stratospheric intrusions may occur.

The along-track cross-section shows that this "super layer" was nearly parallel to the isentropic surfaces between approximately 305K and 320K (Plate 4a). There were relatively high PV patches with values exceeding 5×10^{-7} K $m^2kg^{-1}s^{-1}$ appearing within or near the base of the ozone layer, producing an internal consistency between the lidar ozone and other trace constituents. To illustrate that this layer was originally part of a collision in the troposphere with upper level stratospheric intrusions impacting a polluted Asian outflow, we display the potential vorticity on the 315K isentropic surface (which lies through the middle of the layer as indicated in Plate 4a) at 00Z February 28 when the DC-8 just flew across the dateline in Plate 5a. The mean fields for the period between 00Z February 22 and 18Z March 1 is also shown in Plate 5b. The two-high, one-trough pattern discussed in the previous section again emerged for both panels. The much amplified isentropic PV trough in Plate 5a exhibits a prominent stratospheric intrusion occurring in the middle of the Pacific that began on February 24 (see section 3). Although the DC-8 traversed 15º south of the trough's southern end, the patches of elevated PV encountered by the plane can be found following the strong sourthward or southwestward flow near the eastern sectors of the two subtropic highs. The region inbetween these two highs where the DC-8 traversed around 00Z February 28 was an interesting place. Plate 6

presents the ending points of backward trajectories arriving in the rectangle region (12.5ºN to 22.5ºN, 160ºE to 180º) with 0.5º apart at 700hPa on 00Z February 28, 2001 for (a)0 day, (b)-1 days, (c)-2 days (d)-3 days, (e)-4 days, and (f)-5 days. The pressure height of a point is indicated by the color as shown in the color bar in (a). It is evident that this region might be influenced by the flow directly from the western subtropical high, a retrograde flow from the eastern subtropical high, and also the air from the tropopause folding that we will discuss next. The trajectory traced air parcels that may come from as low as 972hPa surface, and as high as 258hPa.

There is good evidence of tropopause folding when we examine the vertical cross-sections through the upper level trough along three longitudes with 10 degrees apart (namely, 160ºE, 170ºE, and 180º) in Plate 7. Although the classic break in the tropopause can be found near 30ºN at about 250hPa level along 160ºE (Plate 7a), that is, with isotherms of potential temperature tightly spaced in the sloping hyperbaroclinic zone and the stratosphere much lower on the poleward side of jet, it is interesting to notice that another stratospheric intrusion is also evident between 40ºN and 45ºN near 350hPa, with a weak easterly center located north of it. Both folding processes produce a PV tube of large static stability, rich ozone and deficient in water vapor. The same structure can also be found when moving eastward (Plate 7b and 7c) indicating the laminar feature of these tubes. They transport stratospheric properties both southward and downward into low latitudes and altitudes. Although the southern tube seems to intrude more to the lower latitudes and the northern one to penetrate to a lower altitude, we believe that both tubes contribute stratospheric ozone to the elevated ozone concentration found along the flight

track since the isentrops on which these stratospheric air moves are converged near the altitude and latitude of the DC-8.

It is informative to compare the PV and ozone measurements along the flight track. We calculate the along-track PV using a cubic interpolation in space and a linear interpolation in time. Even though the full resolution of the ECMWF data was utilized (section 2.1), one should keep in mind that the resolution for ozone data is far superior than that of PV (horizontal resolution roughly 15km vs. 105km). Figure 4a presents the flight trajectory that varies with height and time (upper panel) with curves of ozone (middle panel) and interpolated PV (bottom panel) as a function of time. The ozone curve show much finer structures than those of the PV curve due to the reason just stated. In general, ozone and PV show a good correlation, with low background values for both quantities corresponding to the part of the flights which is located in the troposphere, and regions of various sizes with higher values, corresponding to intrusions of flight legs in or near the stratosphere.

Stoller et al. [1999] noticed that the presence of layers with ozone and water vapor mixing ratios significantly different from that of the background atmosphere may introduce changes in the radiative heating and cooling rates, which are strongly dependent on these gases. We calculated the radiative heating rate for one particular flight leg along which a quasi-vertical profile was made (the leg is indicated in Figure 4a), using a classic radiative transfer program [Hoffman, 1981]. The largest radiative effect comes from the water vapor element of the layer (see Figure 4b bottom-right panel). There is an enhanced cooling near the layer base (~2 km up to -7˚C per day); the cooling dropped to almost zero near the top of the layer. This radiative tendency

produces stabilization within the layer vertical extension and prevents vertical mixing across it. The fact that the layer was steady at the same altitude for most of its life was another indicator of stability. Although rapid transport may occur around the two subtropical highs in midlatitudes, the stagnant airflow near the southern flanks of these highs reduces the ventilation of the lower atmosphere (Plate 5a and Figure 2a). With the help of the widespread sinking motion within or in the vicinity of these highs, this region may become very "dirty" once the pollutants can reach there under one or two favorable meteorological transport events, as shown for this "super layer" case.

5. Summary and Discussion

One of the principal findings related to the atmospheric structure was that the motions are organized such that characteristic layers occupy much of the space. As for earlier missions we have taken a census of atmospheric layers involving ozone, water vapor, carbon monoxide, and methane. We compared their occurrence with similar layers in previous missions. Their dimensions, including thickness, were quite similar, as was their abundance; they are matched in Table 2. Layers have an average thickness of 0.56 kilometers, heights ranging from 4.9 to 5.8 kilometers, and all together occupying about 21% of the atmosphere. These dimensions are similar to those found earlier. The predominance of the layers from the stratosphere gives an important role to their place in sharing space between the troposphere and the stratosphere. In the literature we have used the four compositions and taken layers of their combinations; but this could easily be expanded by adding different substances. One can go much further and include non-

methane hydrocarbons of different species allowing a good time measurement scale using different mean lifetimes for the separate species. This approach can be extended once the time needed for entry into the stratosphere can be included.

Our analyses for the "super layer" encountered by the DC-8 flight 5 show that this layer was originally part of a collision in the troposphere with an upper level stratospheric layer impacting a polluted layer. We have observed that there were several factors that contributed favorably to the persistence of this layer, i.e., the self-stabilizing effect of a dry layer from a radiative heating perspective; stagnant airflow, and a widespread subsiding atmosphere. We hypothesize here that this "super layer" observation may not be an occasional event. Favorable meteorological settings and events such as the stratospheric folding in conjunction with the surface features can produce a "dirty" layer along the southern flank of oceanic subtropical highs in which the Asian polluted air from sporadic transport can be trapped at low troposphere in this season.

Plate 8 summarizes typical three-dimensional airflow patterns following roughly the isentropic surfaces which accompany tropopause folding and the Asian outflow lifted by WCB. This schematic figure is an extension of *Denielsen* famous chart (figure 12 in his 1980 paper) that depicted only the typical trajectories and deformations associated with a tropopause folding event. It shows that the Asian polluted air can be rapidly transported into the mid-latitude Pacific via WCBs. The plume will split into two branches in central Pacific due to the flow setting: one branch transports air towards tropical region while descending; and the other continuing its transpacific route. The latter one can split further downstream with one sliding down to the low latitudes and the other influencing the North America. All the split branches could be impacted more or

less by the tropopause folding event that pulls down the air of stratospheric origin, as indicated in the Plate. As noted by *Heald et al*. (submitted manuscript, 2003), the Asian pollution layers sampled on the outbound transit DC-8 flights 4 and 5, over a 25º range of latitude (15ºN to 40ºN), were the remnants of a single Asian plume lifted in a WCB over East Asia four days earlier and split by a blocking high. The northern plume continued its transport to North America and was sampled on flight 4, while the southern plume subsided over the tropic Pacific and was sampled on flight 5. All these are clearly fit into our schematic Plate 8. More observations are needed to verify our hypothesis of possible high frequency of dirty layer occurrence in the southern edges of subtropical highs, either through future aircraft survey or satellite measurements.

Numerical model can be a powerful tool in this regard. We have made such an attempt using the Model of Atmospheric Transport and Chemistry (MATCH) three-dimensional off-line model developed at the National Center for Atmospheric Research (NCAR) [*Mahowald et al*., 1997; *Rasch et al.*, 1997]. MATCH contains algorithms for mixing on multiple scales and large-scale precipitation that are identical to those found in the Middle Atmospheric Community Climate Model (MACCM) middle atmospheric model [*Boville and Gent*, 1998; *Kiehl et al*., 1998], also developed at NCAR. Vertical velocities were calculated internally from mass continuity on the model grid. Tracer advection was carried out using a semi-Lagrangian advection scheme [*Rasch and Williamson*, 1990]. We used a pair of tracers in an attempt to diagnose transport within the geographical region of interest for the DC-8 flight 5 during TRACE-P. The first tracer (the "tropospheric tracer") was defined at the surface over lands with an arbitrary mixing ratio of 1 at each time step, with no sinks at the surface (both land and sea) , such that

throughout a model run the mixing ratio at the surface always remained constant. A second tracer (the "stratospheric tracer") was defined in the same manner (constant mixing ratio, no sinks) at levels of 200 hPa and above. Between these two regions transport, mixing, convection, etc., were allowed to change the mixing ratio of either tracers as needed. Preliminary results indicated that the pattern described in the Plate 8 does exist. An example of the result for the mixing ratio of the "stratospheric tracer" is shown in Figure 5. Clearly the tracer has been seeping down from stratosphere into the upper troposphere; and a layer with elevated mixing ratio is identifiable just below 2km (appears lower than the "super layer") for the first half of the mission. Currently we are analyzing the model outputs to give a more detailed picture of the formation of this layer.

Acknowledgments. The MIT contribution to this paper came from NASA grant NCC-1-415.

References

Boville, B. A., and P. R. Gent, The NCAR climate system model version 1, *J. Climate*, 11(6), 1115-1130, 1998.

Browell, E. V., and 22 others, Large-scale air mass characteristics observed over the remote tropical Pacific Ocean during March-April 1999: Results from PEM-Tropics B field experiment, *J. Geophys. Res., 106*, D23, 32,481-32,502, 2001.

Carmichael, G. R., et al.**,** Regional-scale chemical transport modeling in support of intensive field experiments: Overview and analysis of the TRACE-P observations, *J. Geophys. Res.*, *108*(D21), 8823, doi:10.1029/2002JD003117, 2003.

Cho, J., R. E. Newell, B. E. Anderson, J. D. Barrick, and K. L. Thornhill**,** Characterizations of tropospheric turbulence and stability layers from aircraft observations, *J. Geophys. Res.*, *108*(D20), 8784, doi:10.1029/2002JD002820, 2003.

Danielsen, E. F., Report on Project Springfield, DASA Rep. 1517, 97pp., Def. At. Support Agency, Washington, D. C., 1964.

Danielsen, E. F., Stratospheric source for unexpectedly large values of ozone measured over the Pacific Ocean during Gametag, August 1977, *J. Geophys. Res.*, 85(C1), 401-412, 1980.

Danielsen, E. F., R. S. Hipskind, S. E. Gaines, G. W. Sachse, G. L. Gregory and G. F. Hill, Three-dimensional analysis of potential vorticity associated with tropopause folds and observed variations of ozone and carbon monoxide, *J. Geophys. Res.*, 92, 2105-2111, 1987.

Danielsen, E. F., Stratospheric-tropospheric exchange based on radio-activity, ozone and potential vorticity, *J. Atmos. Sci*., 25, 502-518, 1968.

Eluszkiewicz, J., R. A. Plumb, and N. Nakamura, Dynamics of wintertime stratospheric transport in the Geophysical Fluid Dynamics Laboratory SKYHI general circulation model. *J. Geophys. Res*., 100, 20,883-20,900, 1995.

Fuelberg, H. E., C. Kiley, J. R. Hannan, D. J. Westberg, M. A. Avery, and R. E. Newell**:** Meteorological conditions and transport pathways during the transport and chemical evolution over the Pacific (TRACE-P) experiment, *J. Geophys. Res.*, *108*(D20), 8782, doi:10.1029/2002JD003092, 2003.

Hannan, J. R., H. E. Fuelberg, J. Crawford, G. W. Sachse, and D. R. Blake**,** Role of wave cyclones in transporting boundary layer air to the free troposphere during the spring 2001 NASA TRACE-P experiment, *J. Geophys. Res.*, *108*(D20), 8785, doi:10.1029/2002JD003105, 2003.

Holopainen, E. O., L. Rontu, and N. C. Lau, The effect of large-scale transient eddies on the time-mean flow in the atmosphere. J. Atmos. Sci., 39, 1972-1984, 1982.

Holton, J. R., An introduction to dynamic meteorology, 3rd edition, Academic Press, San Diego, CA, 1992.

Jacob, D. J., J. H. Crawford, M. M. Kleb, V. E. Connors, R. J. Bendura, and J. L. Raper, G. W. Sachse, J. C. Gille, L Emmons, and C. L. Heald: Transport and chemical evolution over the Pacific (TRACE-P) aircraft mission: design, execution, and first results, *J. Geophys. Res*., 108(D20), 9000, doi:10.1029/2002JD003276, 2003.

Jackson, D. R., J. Methven, and V. D. Pope, Transport in the low-latitude tropospause zone diagnosed using particle trajectories, *J. Atmos, Sci*., 58, 173-192, 2001.

Kiehl, J. T., J. J. Hack, G. B. Bonan, B. A. Boville, D. L. Williamson, and P. J. Rasch, The National Center for Atmospheric Research Community Climate Model: CCM3, *J. Climate*, 11(6), 1131-1149, 1998.

Kiley, C., et al.**,** An intercomparison and evaluation of aircraft-derived and simulated CO from seven chemical transport models during the TRACE-P experiment, *J. Geophys. Res.*, *108*(D21), 8819, doi:10.1029/2002JD003089, 2003.

Liu, H., D. J. Jacob, I. Bey, R. Yantosca, B. N. Duncan, and G. W. Sachse, Transport pathways for Asian pollution outflow over the Pacific: Interannual and seasonal variations, *J. Geophys. Res.*, *108*(D20), 8786, doi:10.1029/2002JD003102, 2003.

Mahowald, N. M., P. J. Rasch, B. E. Eaton, S. Whittleston, and R. G. Prinn, Transport of ^{222}Radon to the remote troposphere using MATCH and assimilated winds from ECMWF and NCEP/NCAR, *J. Geophys. Res.*, 102, 28,139-28,151, 1997.

Methven, J., Offline trajectories: Calculation and Accuracy, UGAMP Technical Report No. 44, 1997 (Available from CGAM, University of Reading, Earley Gate, Reading, RG6 6BB, United Kingdom).

Newell, R. E., V. Thouret, J. Y. N. Cho, P. Stoller, A. Marenco, and H. G. Smit, Ubiquity of quasi-horizontal layers in the troposphere, *Nature, 398*, 316-319, 1999.

Rasch, P. J., N. M. Mahowald, and B. E. Eaton, Representations of transport, convection, and the hydrologic cycle in chemical transport models: Implications for the modeling of short-lived and soluble species, *J. Geophys. Res.*, 102, 18,127-18,138, 1997.

Stoller, P., J.Y.N. Cho, R.E. Newell, V. Thouret, Y. Zhu, M.A. Carroll, G.M. Albercook, B.E. Anderson, J.D.W. Barrick, E.V. Browell, G.L. Gregory, G.W. Sachse, S. Vay, J.D. Bradshaw and S. Sandholm, Measurements of atmospheric layers from the

NASA DC-8 and P-3B aircraft during PEM-Tropics A, *J. Geophys. Res.*, *104*, D5, 5745-5764, 1999.

Thouret, V., J. Y. N. Cho, R. E. Newell, A. Marenco, and H. G. J. Smit, General characteristics of tropospheric trace constituent layers observed in the MOZAIC program, *J. Geophys. Res.*, 105, 17,379-17,392, 2000.

Thouret, V., J. Y. N. Cho, M. J. Evans, R. E. Newell, M. A. Avery, J. D. W. Barrick, G. W. Sachse, and G. L. Gregory, Tropospheric ozone layers observed during PEM-Tropics B, *J. Geophys. Res.*, 106, 32,527-32,538, 2001.

Wu, C-C., and K. A. Emanuel, Potential vorticity diagnostics of Hurricane Movement. Part I: A case study of Hurricane Bob (1991), *J. Atmos. Sci*.,123, 69-92, 1995.

Figure 1. Water vapor image from GMS satellite for DC-8 flight 5. Flight track is indicated on the image.

Figure 2. (a) Mean sea level pressure (hPa); (b) Upper air maps show 257 hPa geopotential height contours (m) and relative vorticity (10^{-5}/s) in underlying shades of grey (positive cyclonic vorticity in dark colors) for the period between 00Z February 22 to 18Z March 1, 2001. Thick black line indicates the flight track.

Figure 3. Same as Figure 2 except for 12Z February, 2001

Figure 4. (a) DC-8 mission 5 flight track, along-track O_3 mixing ration (ppbv), and potential vorticity ($10^{-7}Km^2kg^{-1}s^{-1}$); (b) Vertical profiles of O_3 (ppbv), CO (ppbv), air/dew-point temperatures (K), and H_2O heating rate (ºC/day) for TRACE-P DC-8 flight 5 around 22:40 UTC, February 27, 2001, near 18ºN, 175ºW.

Figure 5. Along track cross-section of mixing ratio for the "stratospheric tracer" of MATCH. Flight track is indicated by the thick solid line.

Plate 1. Geographical distribution of layers based on ozone and water vapor. Symbols indicate layers with rich O_3 and H_2O (triangles); rich O_3 and poor H_2O (circles);

poor O_3 and rich H_2O (diamonds); poor O_3 and H_2O (squares). Layers are colored according to their altitudes fallen into 1 km bins shown in the color bar.

Plate 2. Same as Figure 1 with each category (based O_3 and H_2O only) displayed separately. Number of observations is indicated on each panel.

Plate 3. Geographical distribution of layers based on O_3, H_2O, CO, and CH_4 for (a) Type 1; (b) Type 2; (c) Type 3; (d) Type 4. Number of observations is indicated on each panel.

Plate 4. Along track cross-section of LIDAR O_3 (color shaded, in ppbv) with (a) potential temperature (in K) and (b) potential vorticity (contours, in 10^{-7} K m^2 kg^{-1} s^{-1}) for TRACE-P DC-8 flight 5 (Kona to Guam). Flight track is indicated by the red line.

Plate 5. (a)Potential Vorticity (shaded, in 10^{-7} K m^2 kg^{-1} s^{-1}), pressure (green contours, in hPa), and streamlines on 315 K isentropic surface at 00Z February 28, 2001. Flight track of DC-8 mission 5 is indicated by the red line; (b) Same as (a) except for mean fields for the period between 00Z February 22 to 18Z March 1, 2001

Plate 6. Ending points of backward trajectories arriving in the rectangle region with 0.5º apart at 700hPa on 00Z February 28, 2001 for (a)0 day, (b)-1 days, (c)-2 days,

(d)-3 days, (e)-4 days, and (f)-5 days. The height of a point is indicated by the color as shown in the color bar in (a).

Plate 7. Vertical cross-sections through the upper level trough along (a)160ºE; (b)170ºE; and (c)180º. Potential Vorticity (shaded, in 10^{-7} K m^2 kg^{-1} s^{-1}), potential temperatures (black contours, in K), and isotachs of zonal wind velocity (green contours, in m s^{-1}) at 00Z February 28, 2001.

Plate 8. Schematic flow pattern associated with a tropopause folding event and Asian polluted outflow

Table 1. Properties of TRACE-P Layers, DC-8 and P-3 Aircraft, for H_2O, O_3, CO, CH_4

Type	Tracer	Obs	PC	Obs/km	h km	p hPa	ΔH km	Δp hpa	ΔH_2O %	ΔO_3 ppbv	ΔCO ppbv	ΔCH_4 ppbv
1A	$+O_3+H_2O+CO+CH_4$	22	7	0.02	5.5	531	0.59	41.4	24.4	18.7	58.9	23.1
1B	$+O_3+H_2O+CO-CH_4$	2	1	0.00	5.4	522	0.25	18.1	10.9	28.3	42.2	-16.0
1C	$+O_3+H_2O-CO+CH_4$	4	1	0.00	6.7	449	0.45	29.9	10.5	16.9	-18.6	12.0
1D	$+O_3+H_2O-CO-CH_4$	9	3	0.01	5.1	535	0.57	42.9	16.7	16.0	-16.8	-12.8
2A	$+O_3-H_2O+CO+CH_4$	74	23	0.06	4.9	560	0.58	41.3	-22.3	21.1	37.9	20.4
2B	$+O_3-H_2O+CO-CH_4$	15	5	0.01	5.7	512	0.66	41.6	-25.3	21.9	14.2	-13.2
2C	$+O_3-H_2O-CO+CH_4$	25	8	0.02	4.8	565	0.47	33.6	-15.0	22.1	-13.9	13.0
2D	$+O_3-H_2O-CO-CH_4$	69	22	0.06	5.4	521	0.59	39.3	-20.1	26.7	-21.1	-17.5
3A	$-O_3+H_2O+CO+CH_4$	16	5	0.01	5.3	537	0.36	23.3	34.0	-14.5	36.1	20.7
3B	$-O_3+H_2O+CO-CH_4$	5	2	0.00	4.5	592	0.26	19.1	21.0	-13.8	16.8	-7.4
3C	$-O_3+H_2O-CO+CH_4$	9	3	0.01	6.4	460	0.73	42.7	22.8	-14.9	-18.1	14.5
3D	$-O_3+H_2O-CO-CH_4$	20	6	0.02	4.5	583	0.53	37.4	20.7	-16.9	-31.0	-17.2
4A	$-O_3-H_2O+CO+CH_4$	9	3	0.01	5.7	504	0.38	24.0	-13.5	-17.9	15.6	11.4
4B	$-O_3-H_2O+CO-CH_4$	6	2	0.00	4.8	571	0.62	39.1	-10.3	-19.8	18.8	-10.8
4C	$-O_3-H_2O-CO+CH_4$	9	3	0.01	5.8	405	0.78	52.9	-22.2	-17.7	-18.2	14.5
4D	$-O_3-H_2O-CO-CH_4$	21	7	0.02	5.1	540	0.70	47.9	-19.2	-17.1	-44.1	-16.3
Average		315		0.25	5.2	538	0.57	38.8	21.0	20.8	29.2	17.2

Table 2. Occurrence and characteristics of atmospheric layers.
(a) Percentage of layer types for different missions.

	$-O_3/+H_2O$	$+O_3/-H_2O$	$-O_3/+H_2O$	$-O_3/-H_2O$
PEMA	14	54	15	18
PEMB	11	54	17	18
PEMTA	12	53	19	17
PEMTB	7	68	9	16
MOZAIC	15	50	17	18
TRACE-P	13	55	17	16

(b) Number, thickness, and height for layer types.

	$-O_3/+H_2O$			$+O_3/-H_2O$			$-O_3/+H_2O$			$-O_3/-H_2O$		
	No.	Th.*	Ht.*	No.	Th.	Ht.	No.	Th.	Ht.	No.	Th.	Ht.
PEMA	11	0.68	5.7	43	0.76	5.2	12	0.87	5.1	14	0.86	6.5
PEMB	8	0.59	6.5	38	0.99	6.0	12	0.64	6.0	13	0.49	6.4
PEMTA	27	0.45	6.0	120	0.71	5.2	43	0.47	5.4	38	0.45	6.1
PEMTB	14	0.40	6.6	133	0.49	5.6	18	0.92	7.6	31	0.57	7.2
MOZAIC	3,341	0.67	6.3	11,288	0.86	5.7	3,751	0.78	5.8	4,000	0.74	5.9
TRACE-P	60	0.46	4.9	254	0.58	5.3	79	0.56	5.2	73	0.59	5.8

* Thickness(Th.) and hight (Ht.) in km.

(c) Percentage of atmosphere occupied by layers.

	Profiles (km)	Ave. Thickness (km)	Total no. of layers	% Occupied
PEMA	439	0.78	80	14
PEMB	388	0.79	71	14
PEMTA	655	0.59	228	20
PEMTB	1330	0.54	196	8
MOZAIC	105,498	0.79	22,380	17
TRACE-P	1254	0.56	466	21

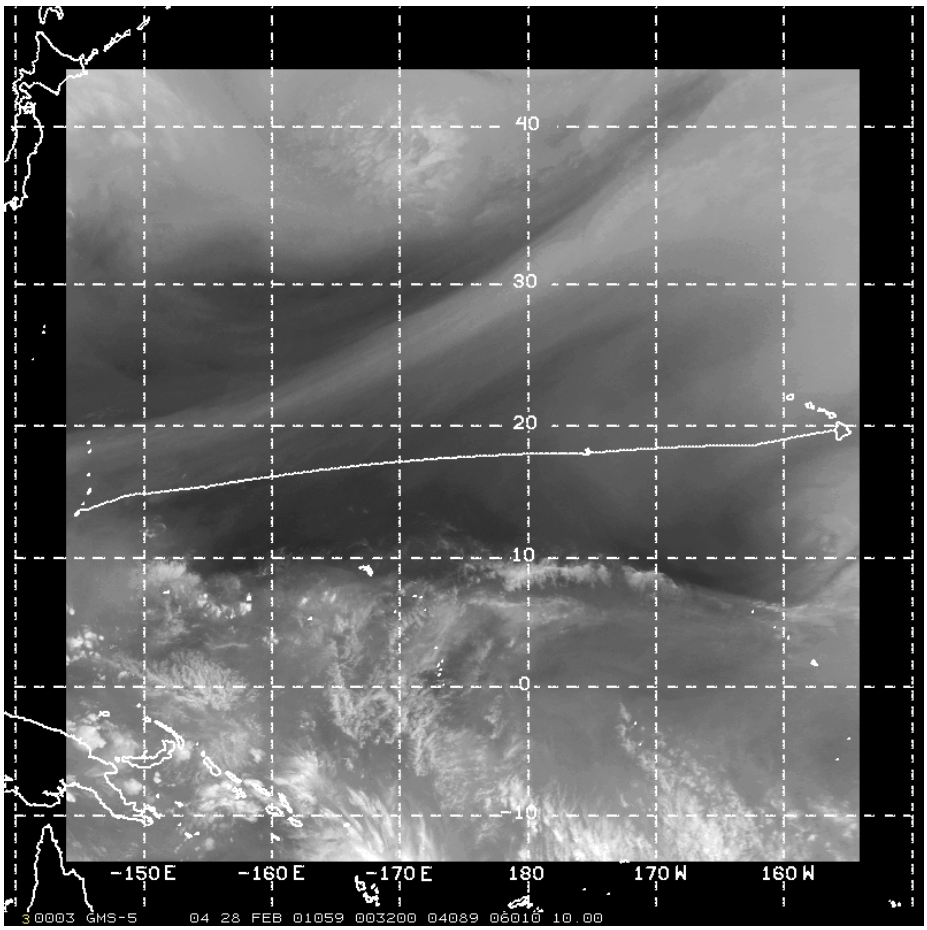

Figure 1. Water vapor image from GMS satellite for DC-8 flight 5. Flight track is indicated on the image.

(a)

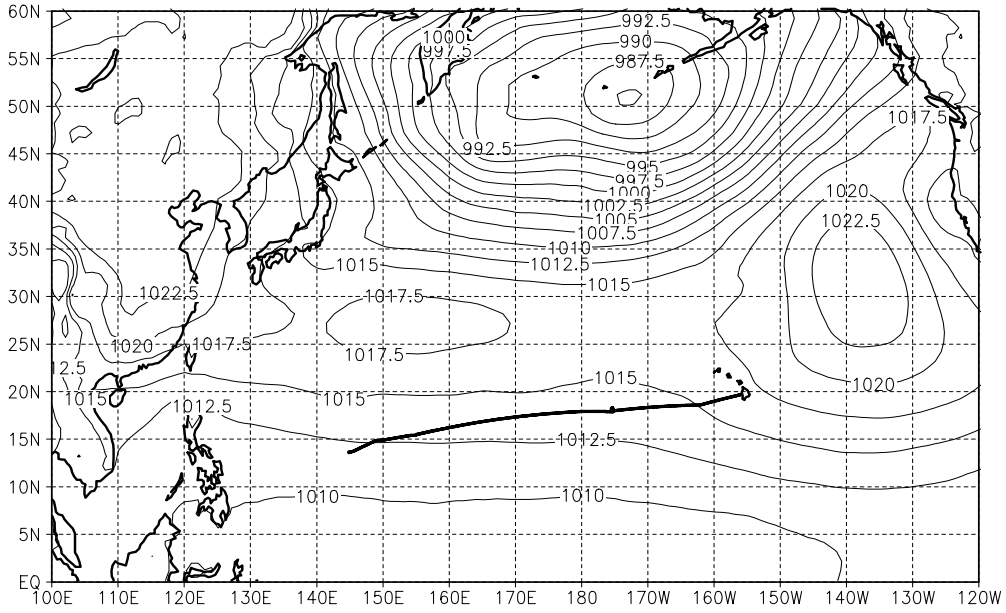

(b)

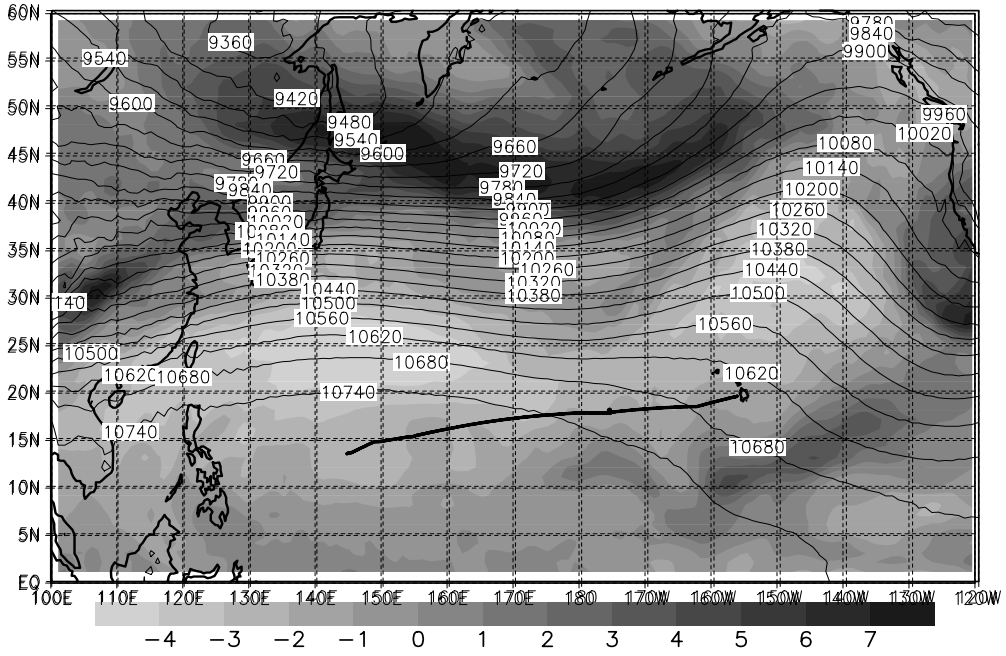

Figure 2. (a) Mean sea level pressure (hPa); (b) Upper air maps show 257 hPa geopotential height contours (m) and relative vorticity (10^{-5}/s) in underlying shades of grey (positive cyclonic vorticity in dark colors) for the period between 00Z February 22 to 18Z March 1, 2001. Thick black line indicates the flight track.

(a)

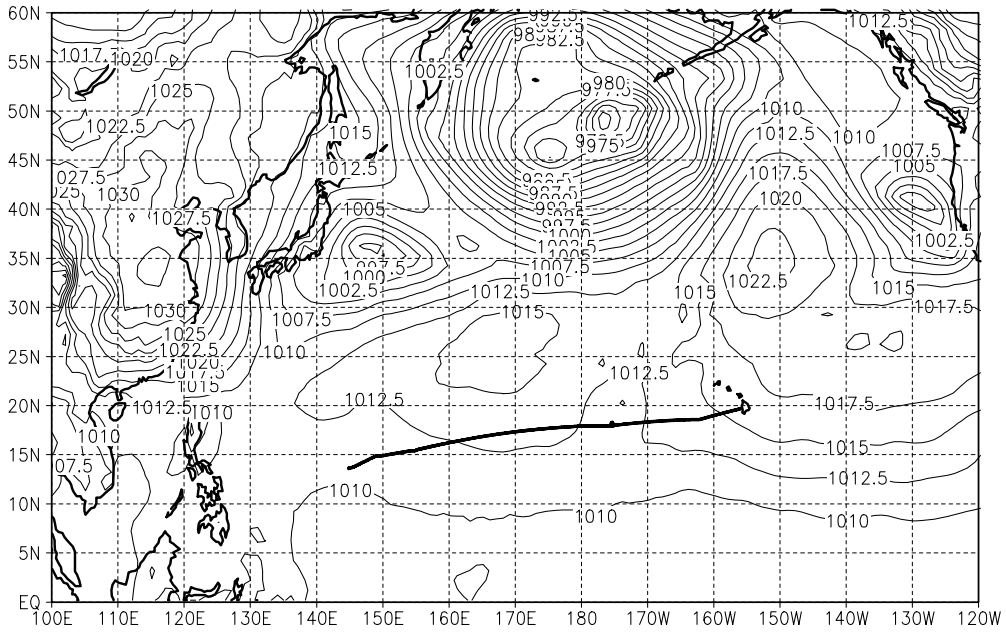

(b)

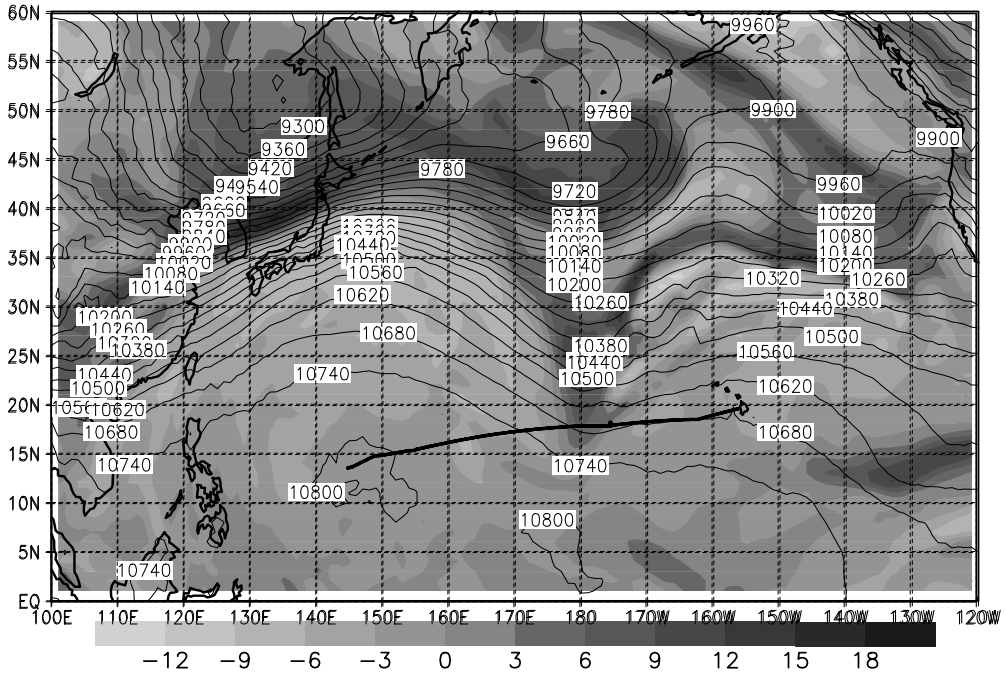

Figure 3. Same as Figure 2 except for 12Z February, 2001

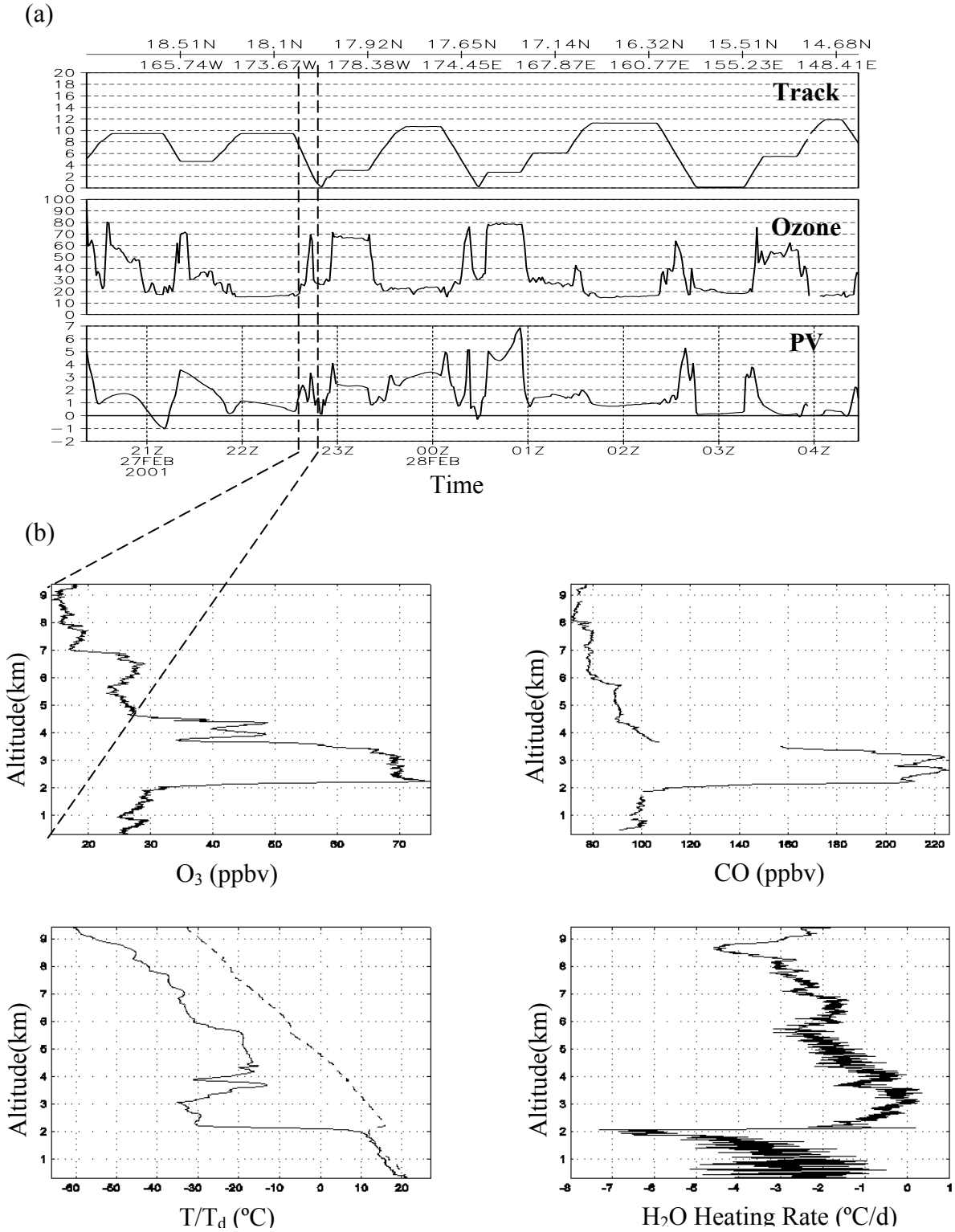

Figure 4. (a) DC-8 mission 5 flight track, along-track O_3 mixing ration (ppbv), and potential vorticity (10^{-7}Km^{2}kg^{-1}s^{-1}); (b) Vertical profiles of O_3 (ppbv), CO (ppbv), air/dew-point temperatures (K), and H_2O heating rate (ºC/day) for TRACE-P DC-8 flight 5 around 22:40 UTC, February 27, 2001, near 18ºN, 175ºW.

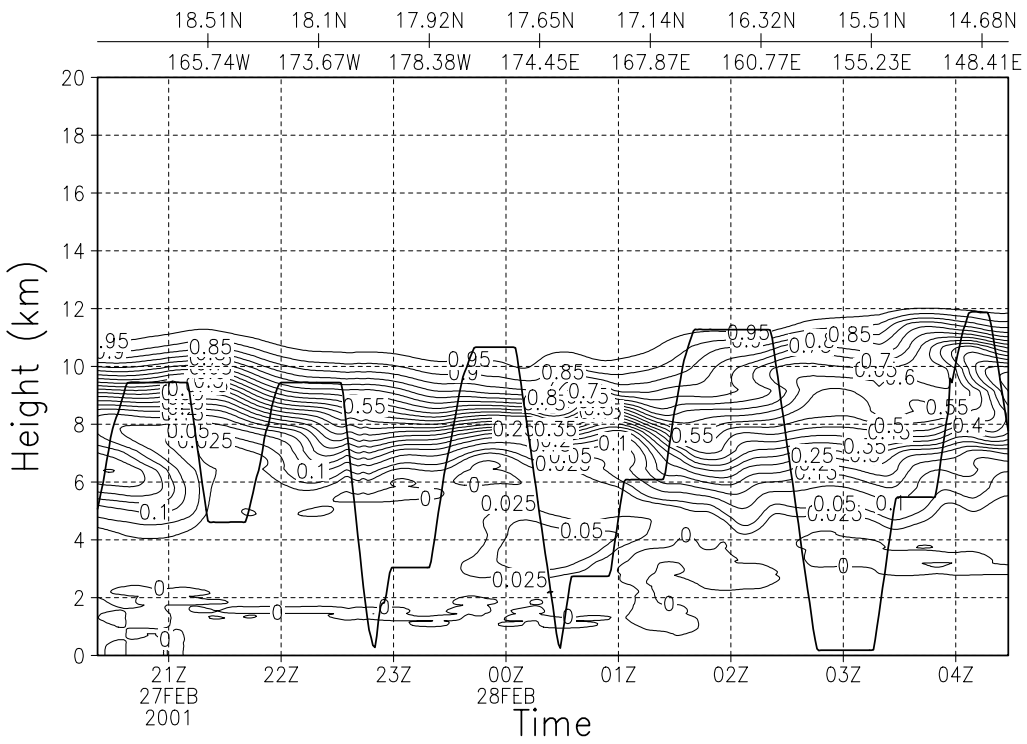

Figure 5. Along track cross-section of mixing ratio for the "stratospheric tracer" of MATCH. Flight track is indicated by the thick solid line.

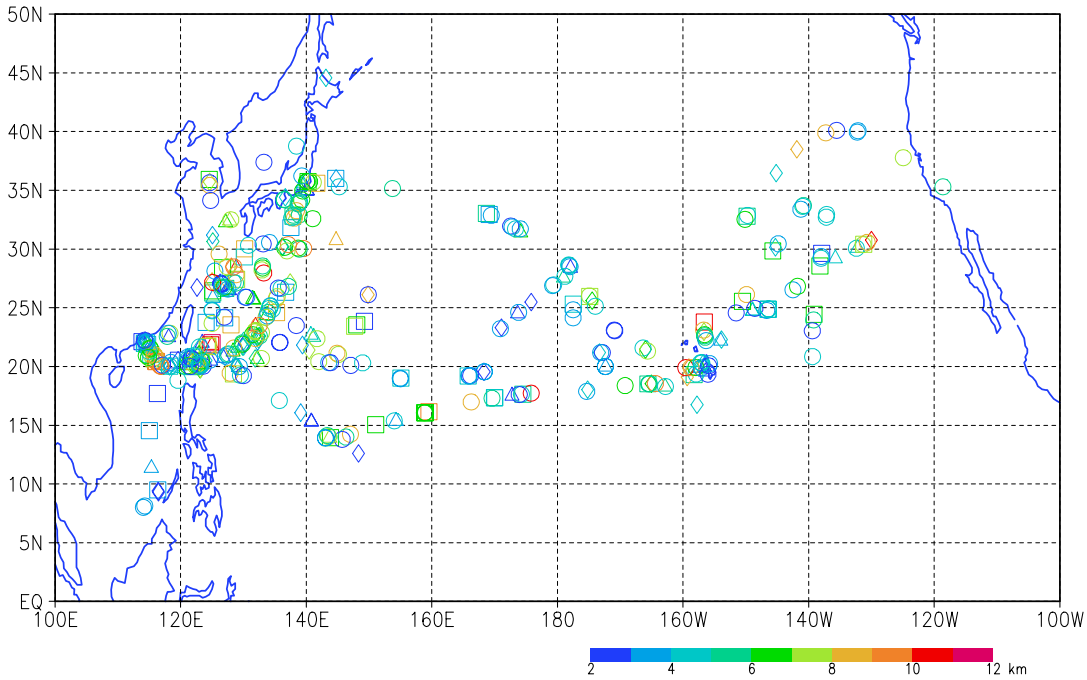

Plate 1. Geographical distribution of layers based on ozone and water vapor. Symbols indicate layers with rich O_3 and H_2O (triangles); rich O_3 and poor H_2O (circles); poor O_3 and rich H_2O (diamonds); poor O_3 and H_2O (squares). Layers are colored according to their altitudes fallen into 1 km bins shown in the color bar.

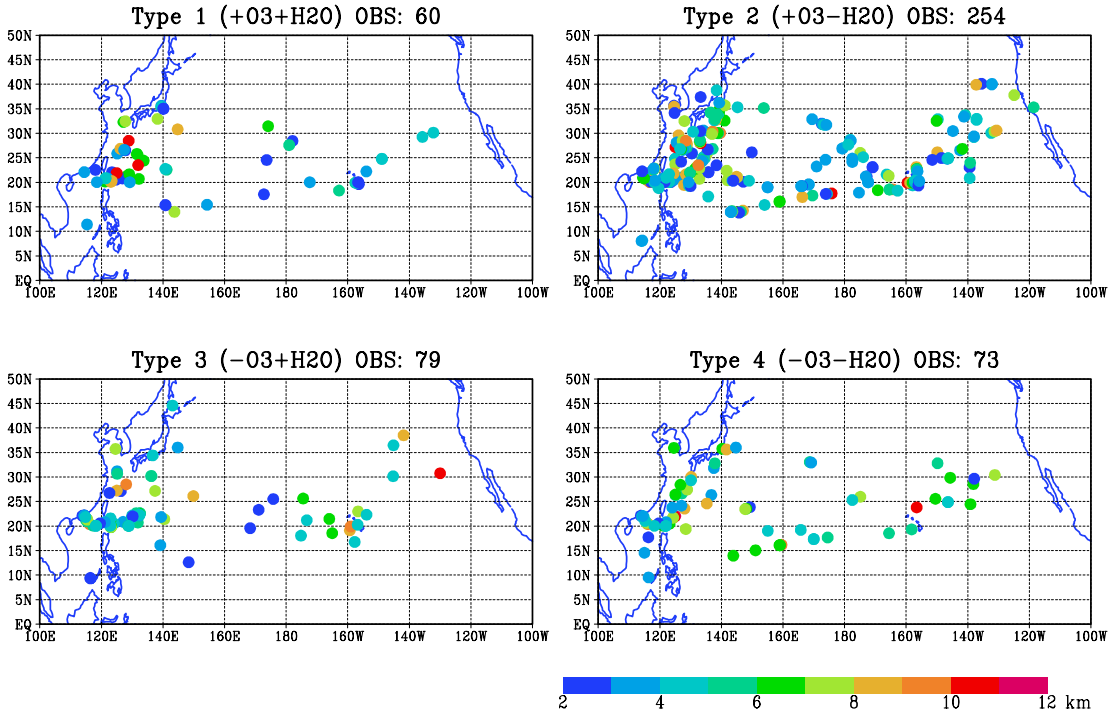

Plate 2. Same as Figure 1 with each category (based O_3 and H_2O only) displayed separately. Number of observations is indicated on each panel.

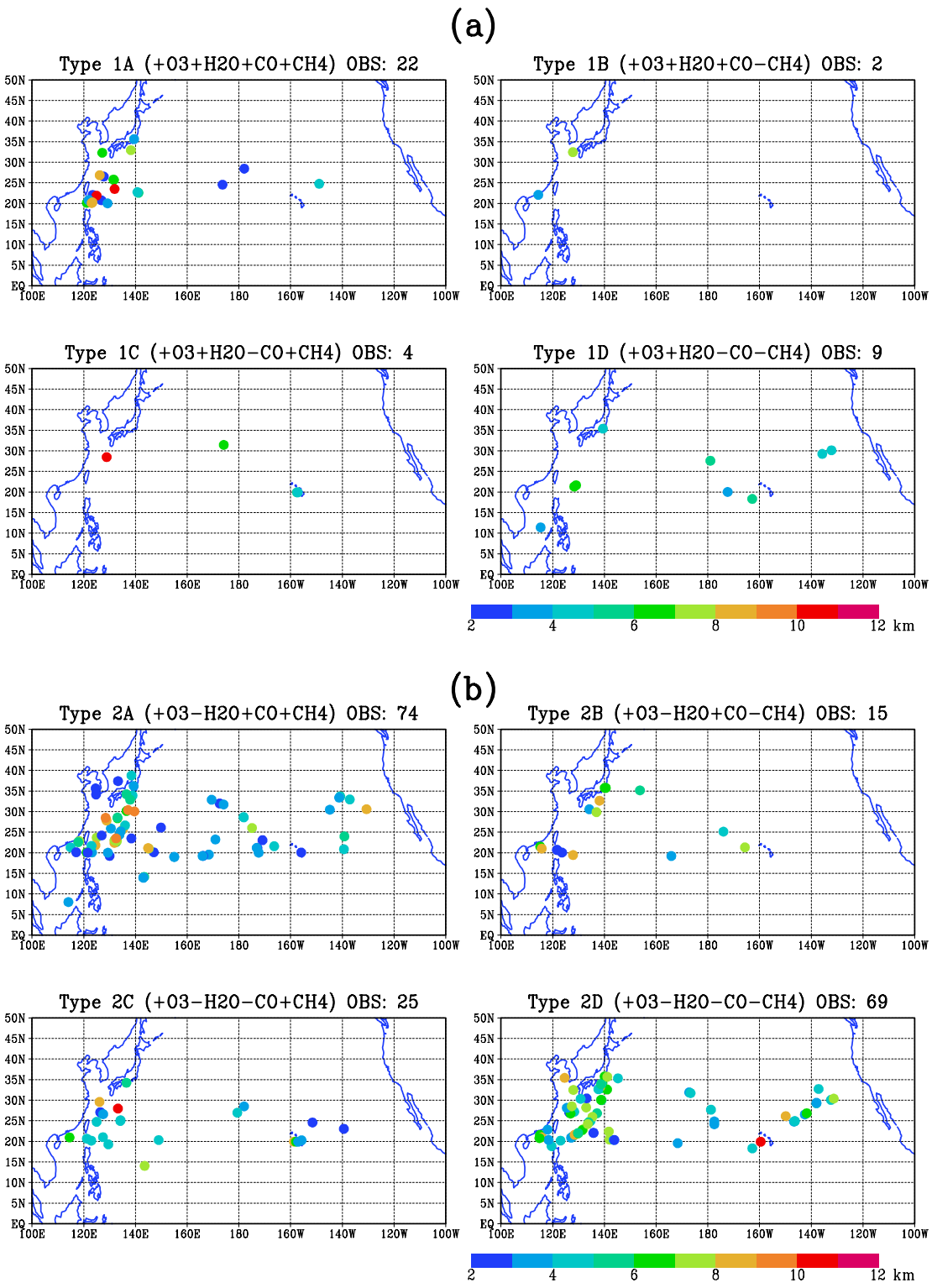

Plate 3. Geographical distribution of layers based on O_3, H_2O, CO, and CH_4 for (a) Type 1; (b) Type 2; (c) Type 3; (d) Type 4. Number of observations is indicated on each panel.

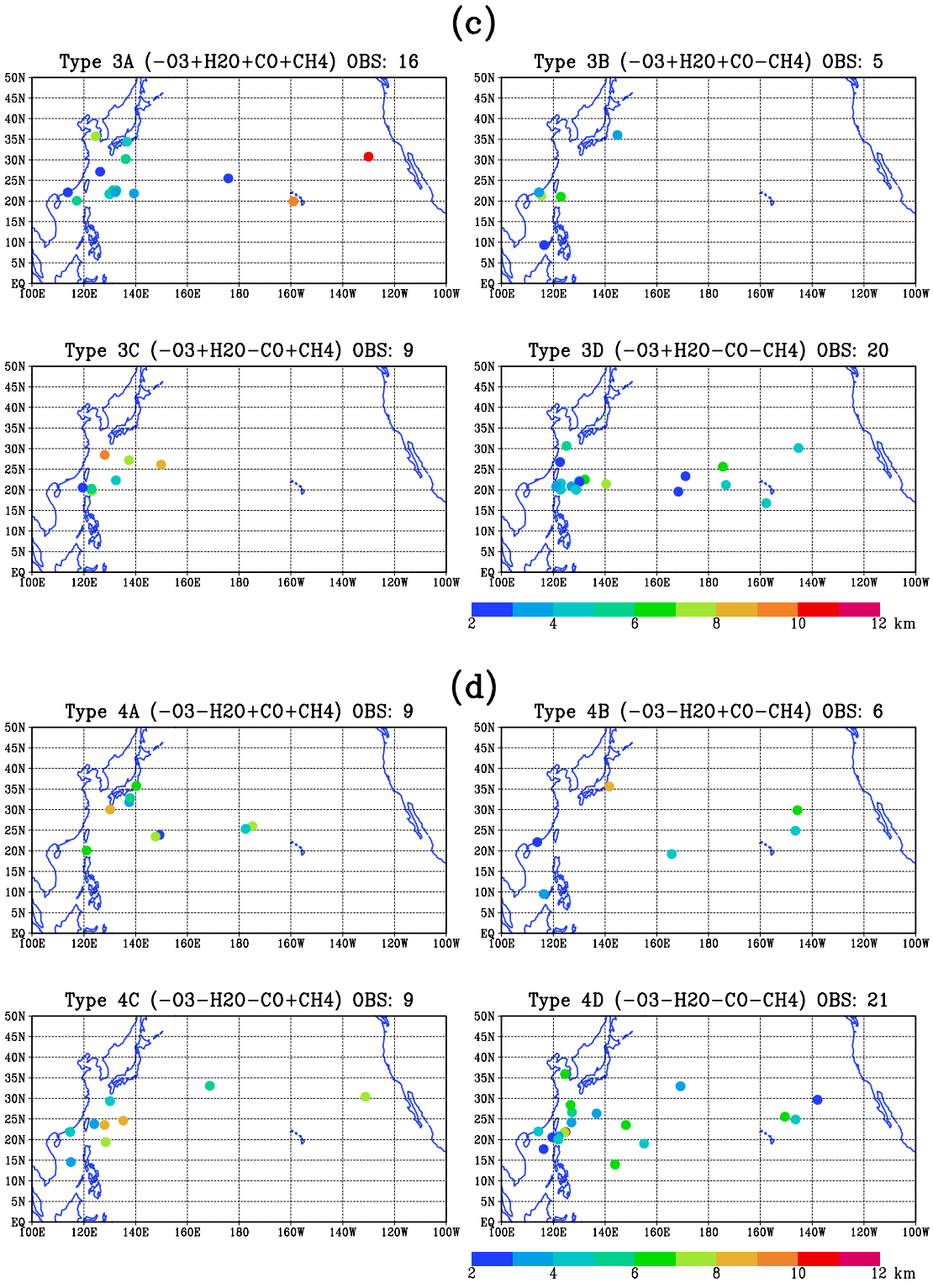

Plate 3. (*Continued*)

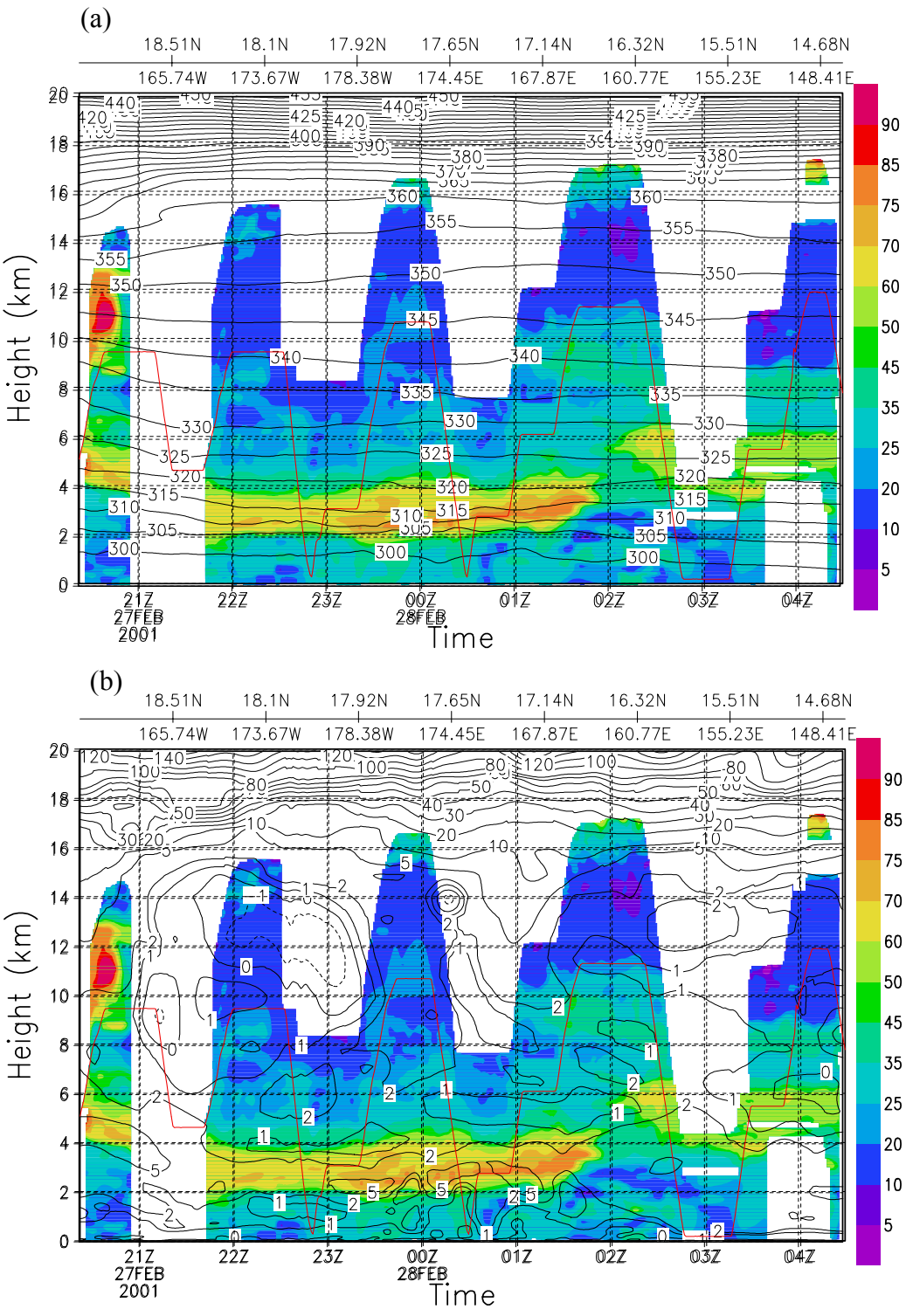

Plate 4. Along track cross-section of LIDAR O_3 (color shaded, in ppbv) with (a) potential temperature (in K) and (b) potential vorticity (contours, in 10^{-7} K m^2 kg^{-1} s^{-1}) for TRACE-P DC-8 flight 5 (Kona to Guam). Flight track is indicated by the red line.

(a)

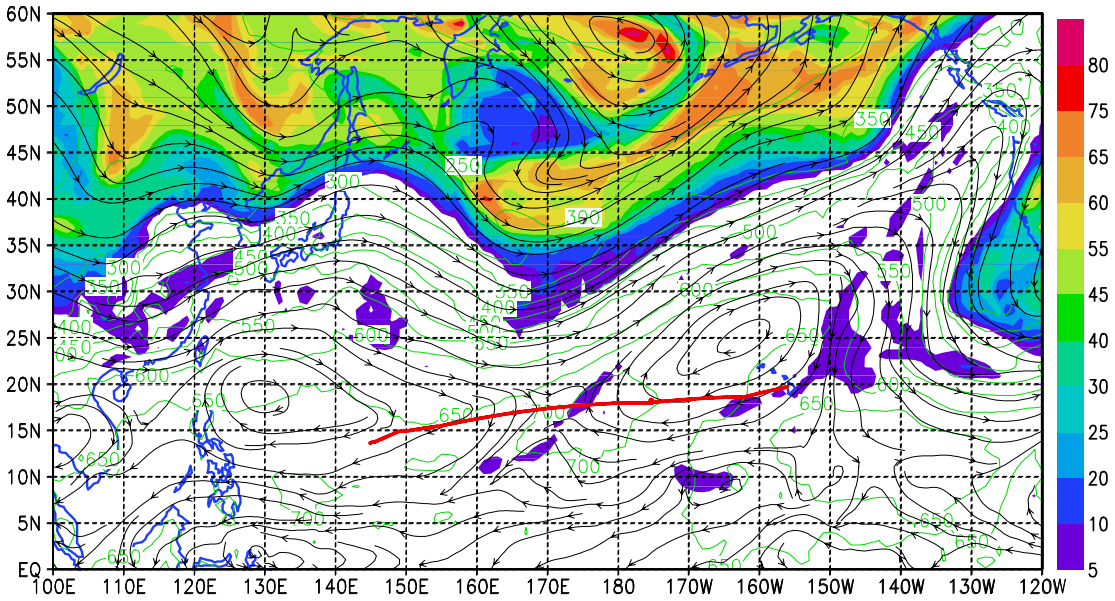

(b)

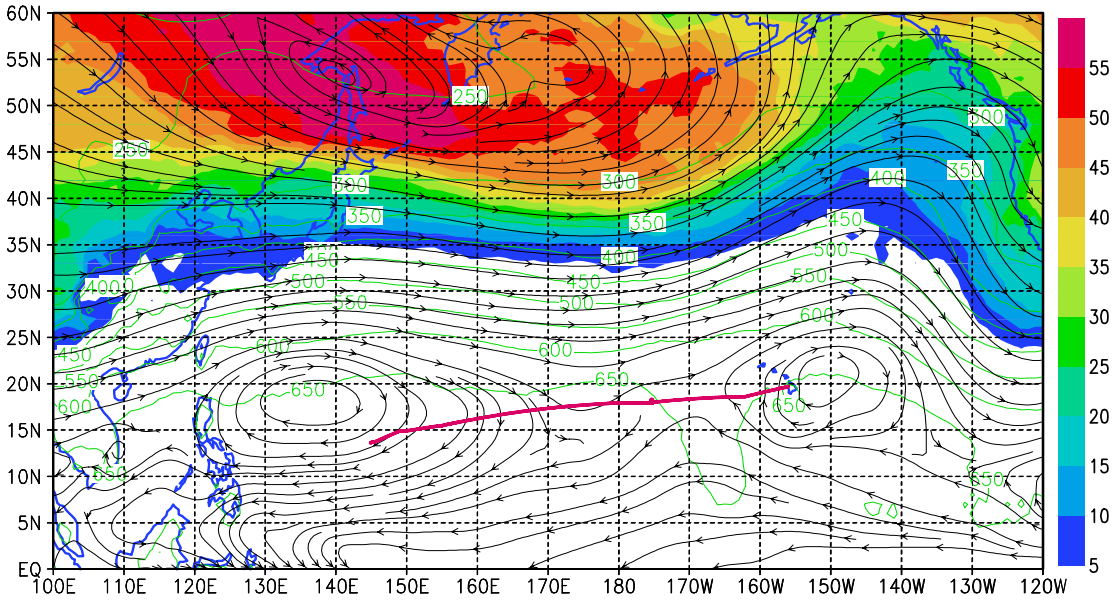

Plate 5. (a)Potential Vorticity (shaded, in 10^{-7} K m^2 kg^{-1} s^{-1}), pressure (green contours, in hPa), and streamlines on 315 K isentropic surface at 00Z February 28, 2001. Flight track of DC-8 mission 5 is indicated by the red line; (b) Same as (a) except for mean fields for the period between 00Z February 22 to 18Z March 1, 2001

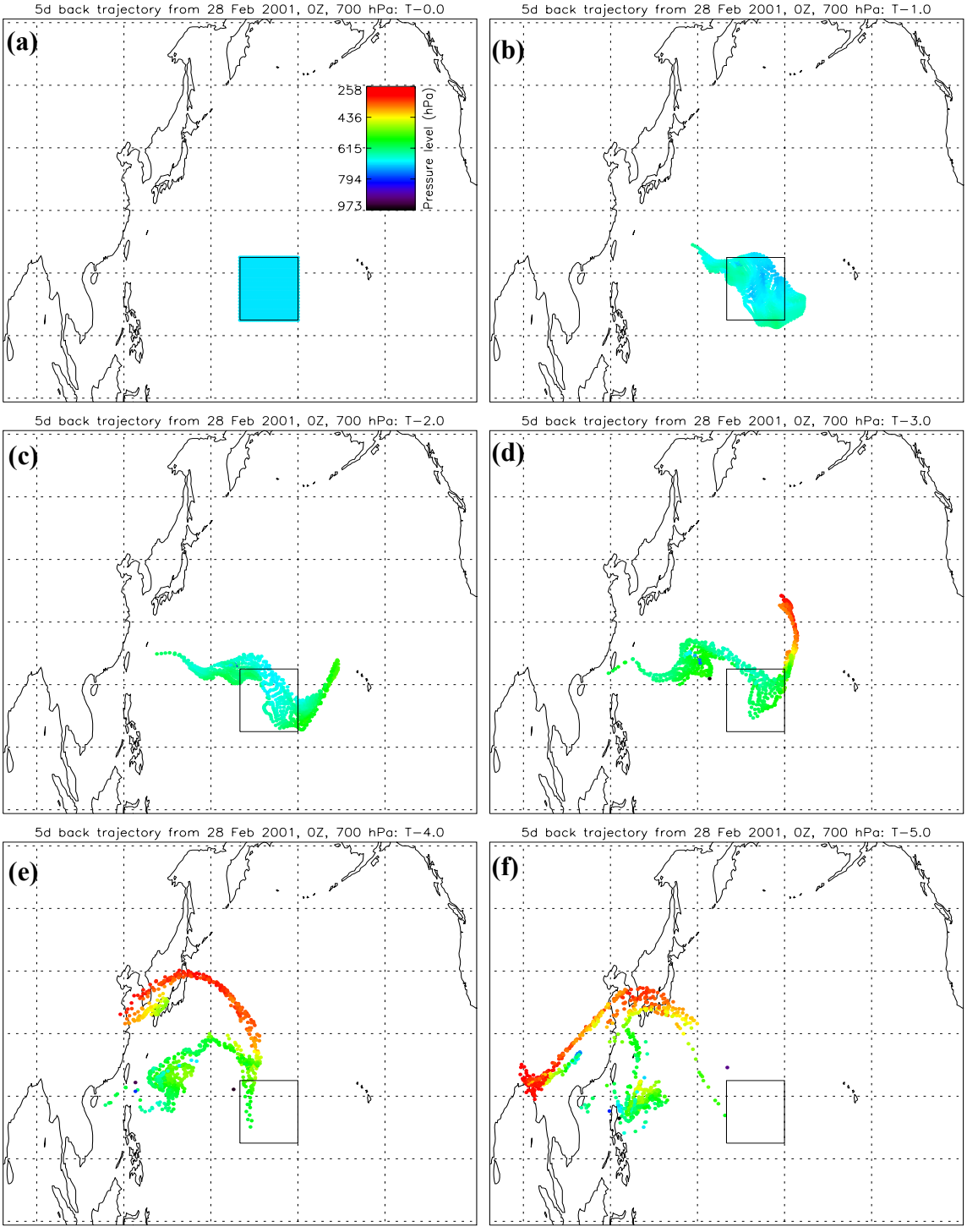

Plate 6. Ending points of backward trajectories arriving in the rectangle region with 0.5º apart at 700hPa on 00Z February 28, 2001 for (a)0 day, (b)-1 days, (c)-2 days, (d)-3 days, (e)-4 days, and (f)-5 days. The height of a point is indicated by the color as shown in the color bar in (a).

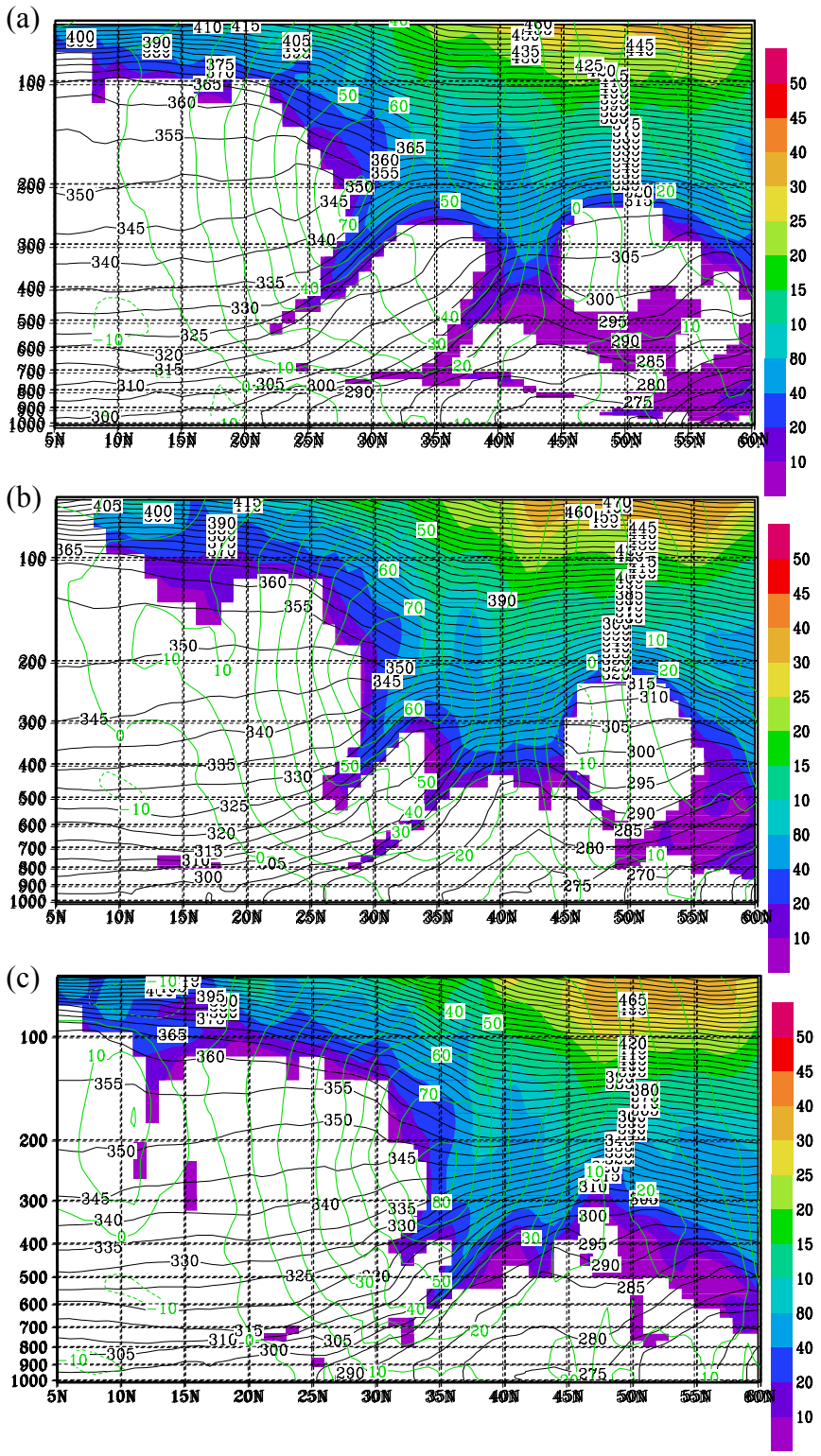

Plate 7. Vertical cross-sections through the upper level trough along (a)160ºE; (b)170ºE; and (c)180º. Potential Vorticity (shaded, in 10^{-7} K m^2 kg^{-1} s^{-1}), potential temperatures (black contours, in K), and isotachs of zonal wind velocity (green contours, in m s^{-1}) at 00Z February 28, 2001.

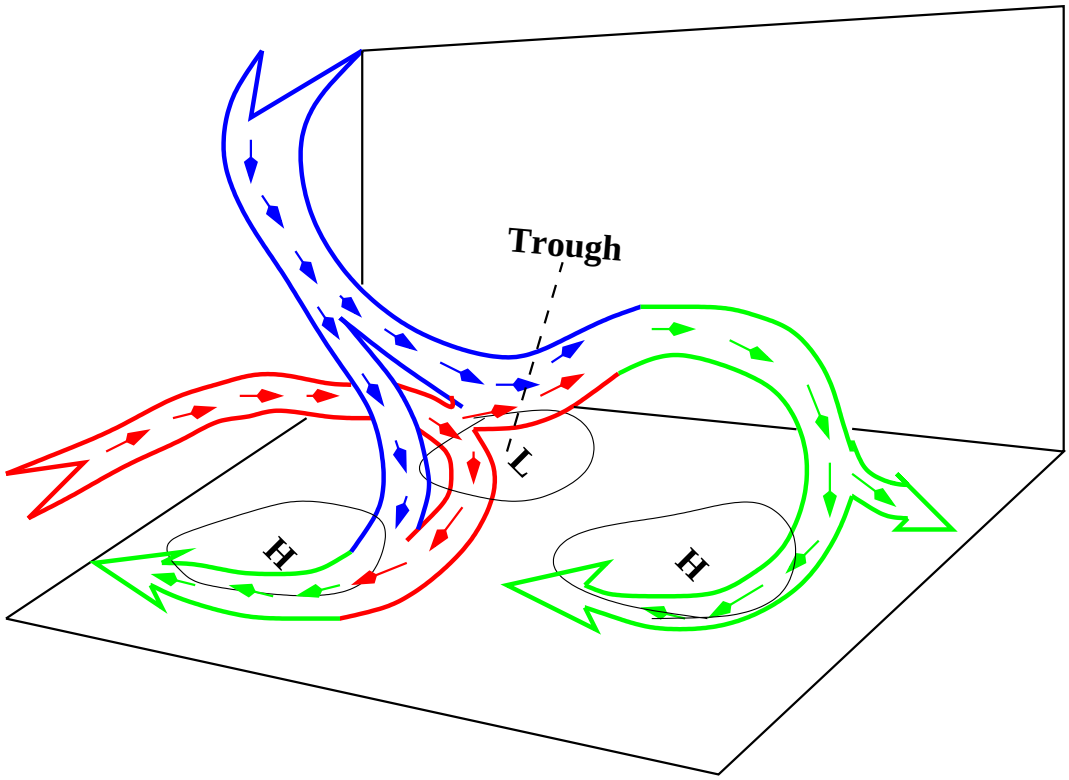

Plate 8. Schematic flow pattern associated with a tropopause folding event and Asian polluted outflow